Kinematic Edge Detection Using Finite Impulse Response Filters

ILD Publication Report

Madalina Chera

ILD General Meeting, 5th of February 2019

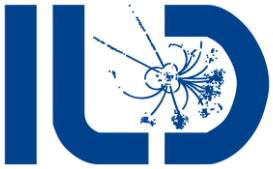

Organisational Overview

- Paper title: "*Kinematic Edge Detection Using Finite Impulse Response Filters*"
- Authors: M. Berggren, S. Caiazza, M. Chera, J. List
- Publication based on two PhD theses (Univ. Hamburg & DESY):
  - S. Caiazza – "*The GridGEM module: a new GEM based readout module for a large TPC & A new algorithm for the determination of the position of kinematic edges in SUSY decays*", DOI: 10.3204/PUBDB-2018-05289
  - M. Chera – "*Particle Flow: From First Principles to Gaugino Property Determination at the ILC*", DOI: 10.3204/PUBDB-2018-01897
- To be submitted to "***Nuclear Instruments and Methods in Physics - A***"
- **ILD internal reviewers**: **Daniel Jeans** and **Remi Ete** – many thanks!
- Current status: 22 pages + bibliography, 2 subsections awaiting completion (aim to be ready before ILD meeting, 26-27 February)
- Last comprehensive presentation to ILD on 3rd of July 2018
  ⇒ **this talk: only most recent changes and updates**

Paper Overview

- Many observables determined from differential features in experimental data distributions → main focus: edge positions in kinematic distributions
- "Traditional" approaches:
  - describe measured spectrum with well motivated function ↔ requires a priori assumptions and approximations
  - compute (numerically) first derivative of distribution ↔ highly sensitive to noise (e.g., detector resolution, beam energy spectrum, intrinsic particle width)
- We propose a new method that circumvents these issues:
  apply a Finite Impulse Response (FIR) filter on the measured spectra
- Method already used in signal processing. Feasible for HEP & discrete input data?
  - Reformulate (Canny's) optimisation criteria for discrete domain
  - Demonstrate that *first derivative of Gaussian* performs best
- Consider two complementary study cases accessible at ILC @ $\sqrt{s}$ = 500 GeV, $P(e^-)$ = -80%, $P(e^+)$ = +30%, $\int$Ldt = 500 fb^{-1}:
  - **STC4:** Phys. Rev. D. 88, 055004 (s-electron pair production)
  - **"Point 5":** arXiv:hep-ex/0603010v1 (gaugino pair production)
- FIR method significantly more robust to fluctuations and even more precise!

Paper Outline

1. Introduction
2. A Computational Approach to Edge Detection
    1. Optimisation Criteria for a Discrete Function Edge Finder
    2. Systematic uncertainties
3. Study Cases
    1. The STC4 Scenario
    2. The “Point 5” Scenario
4. Measurement of the $\tilde{e}$ and $\tilde{\chi}_1^0$ masses at the ILC
5. Edge Measurements with FIR Filters in the Point 5 Study Case
6. Conclusions

Section 2: Main Changes

A Computational Approach to Edge Detection

- Introduced **new figures**:

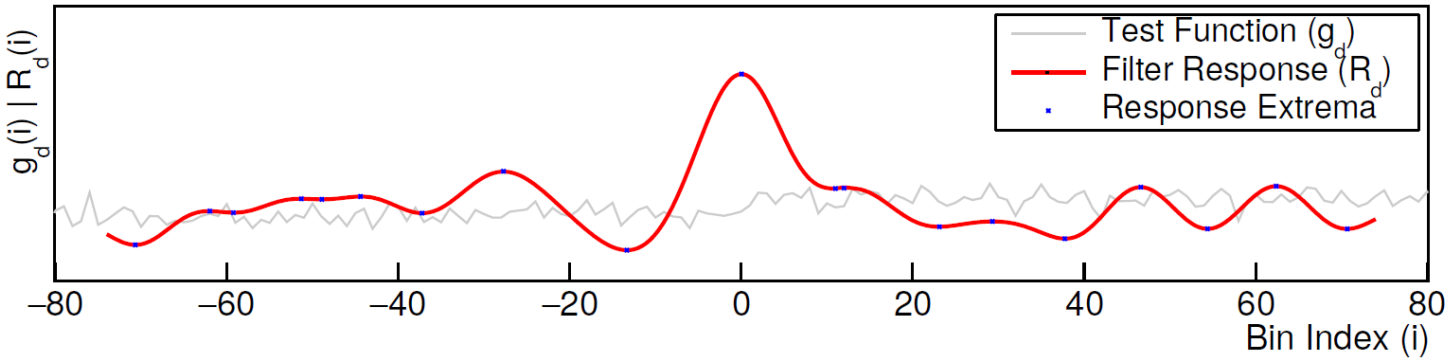

Figure 1: Example of the application of the edge finding algorithm to a noisy step function with a signal-to-noise ratio of 1.0. The test function to which the algorithm is applied is obtained applying overlaying a white-noise of $\sigma = 1$ to an ideal step function of amplitude $A = 1$ at $i = 0$. We processed the test function with a FDOG filter with $\sigma_f = 5$. Using our algorithm the maximum positive response, identifying the step position was detected at $x = 0.04$

Section 2: Main Changes

A Computational Approach to Edge Detection

- Introduced **new figures**:

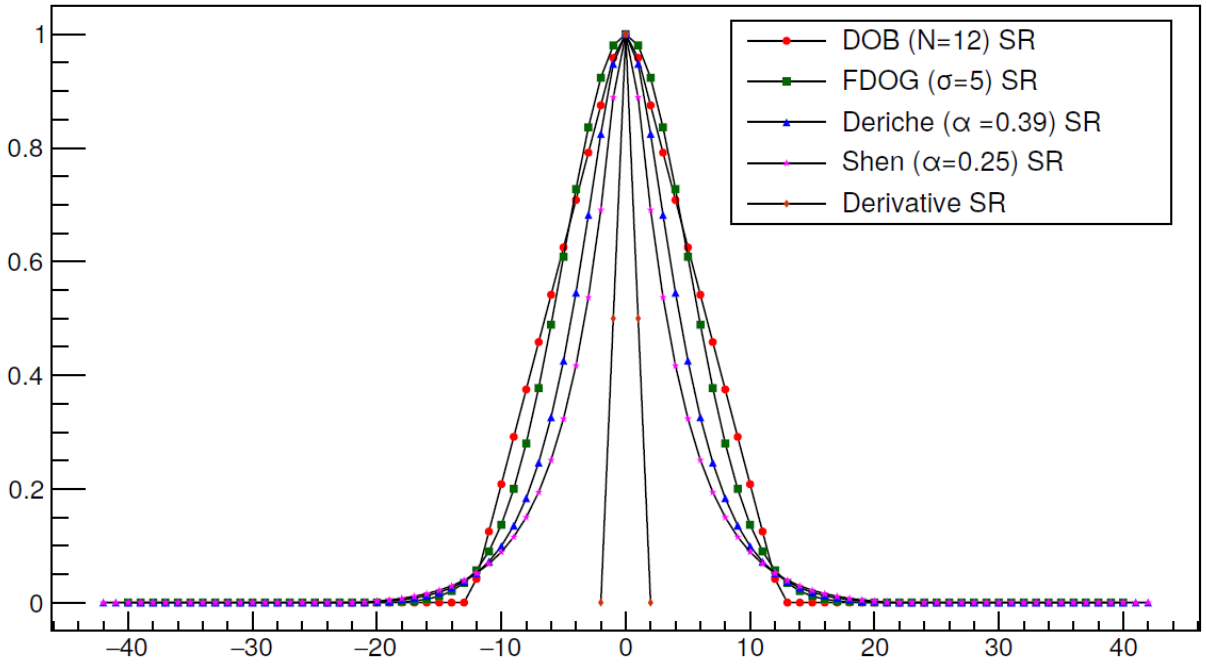

Figure 2: Normalized step response function of the 4 studied filters, as compared with the response of the numerical derivative. The characterizing parameter of each filter was chosen so that they will have a scale factor of about 5 to make a comparison more meaningful.

(will be remade to conform to ILD style)

Section 2: Status

A Computational Approach to Edge Detection

- Remaining figures will be remade according to ILD graphics style

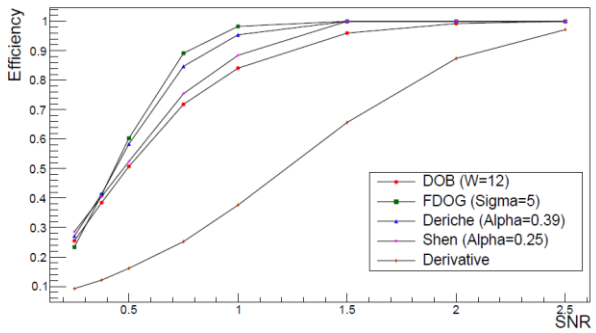

Figure 3: The efficiency of four different filters, compared to that of the traditional derivative for varying Signal-to-Noise-Ratio on a step function (width = 1). A random peak choice would result in an efficiency of about 5%. The size of all filters is about 5.

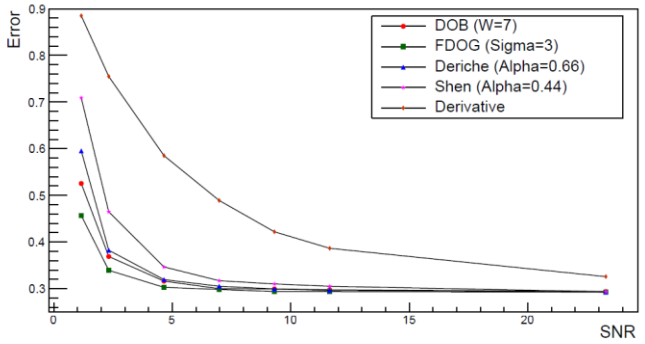

Figure 4: The localization error of different filters of similar size (≈ 3) is calculated on a smooth step of fixed size ($W = 10$) with changing Signal-to-Noise-Ratio.

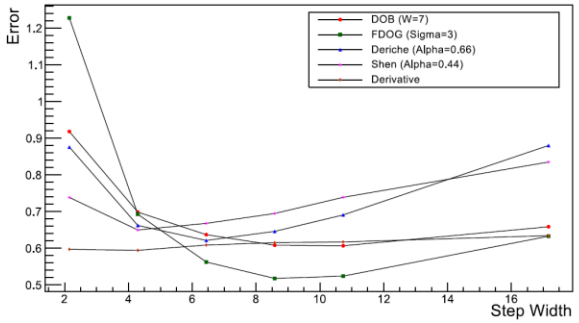

Figure 5: The localization error of different filters of similar size, is calculated on a smooth step function with fixed $S/N = 0.5$, plotted in this figure for a variable step width. At low S/N the presence of an optimal filter size is particularly evident but this characteristic is generally present for any value of S/N

Section 3: Main Changes

Study Cases

- Included formulae explaining mass calculation from kin. edge positions
- Introduced **new figure** (based on ILD full simulation DBD Monte Carlo data):

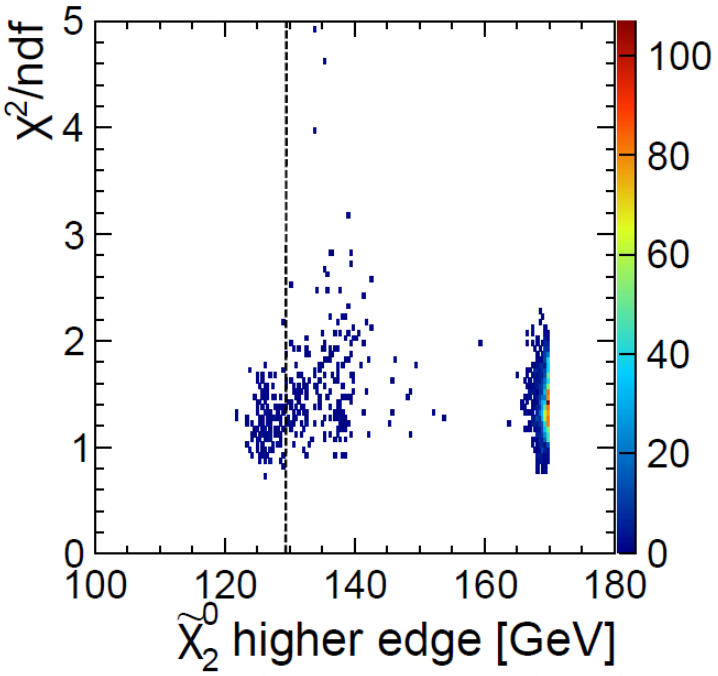

Figure 6: Results of the toy Monte Carlo study performed to evaluate the consistency of the fitting method for kinematic edge extraction. The number of converged fits is illustrated by the colour code. The black, dashed vertical line shows the location of the model calculated edge.

Section 4: Status

Measurement of the $\tilde{e}$ and $\tilde{\chi}_1^0$ masses at the ILC

- Requires text to be finalised
- Current figures based on ILD - SGV DBD Monte Carlo data (will be remade according to ILD graphics style):

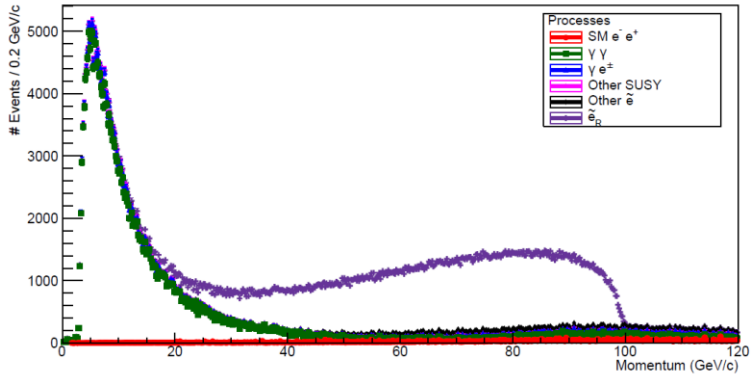

Figure 7: J_H momentum distribution at the end of the high-momentum edge selection. That distribution will be used as a template to calculate the position of the high-momentum edge and the error correlated to that measurement.

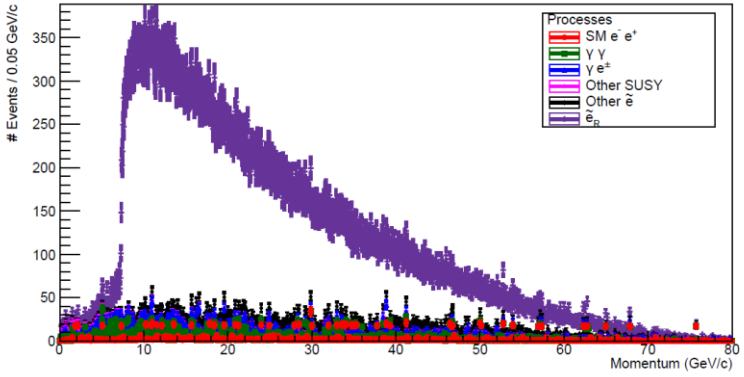

Figure 8: Distribution of the J_L momentum after the application of the low-momentum edge selection described in the text. This distribution will be used as a template to calculate the position of the low-momentum edge and the error correlated to that measurement

Section 4: Final Results

Measurement of the $\tilde{e}$ and $\tilde{\chi}_1^0$ masses at the ILC

- Measured edges:

	Lower edge [GeV]	Upper Edge [GeV]
Calculated	7.298	99.362
Measured	7.409 ± 0.012	98.748 ± 0.043

- Perform edge calibration:

	Lower edge [GeV]	Upper Edge [GeV]
Calibrated	7.300 ± 0.012 ⊕ 0.042	99.349 ± 0.043 ⊕0.008

- Final calculated masses:

	Mass $\tilde{\chi}_1^0$ [GeV]	Mass $\tilde{e}$ [GeV]
FIR filter edges	95.56 ± 0.09	126.20 ± 0.11
arxiv: 1508.04383	95.47 ± 0.16	126.20 ± 0.21
STC4 model	95.58	126.24

Section 5: Status

Edge Measurements with FIR Filters in the Point 5 Study Case

- Text is ready for review
- All figures produced with ILD – DBD full simulation Monte Carlo data (final)

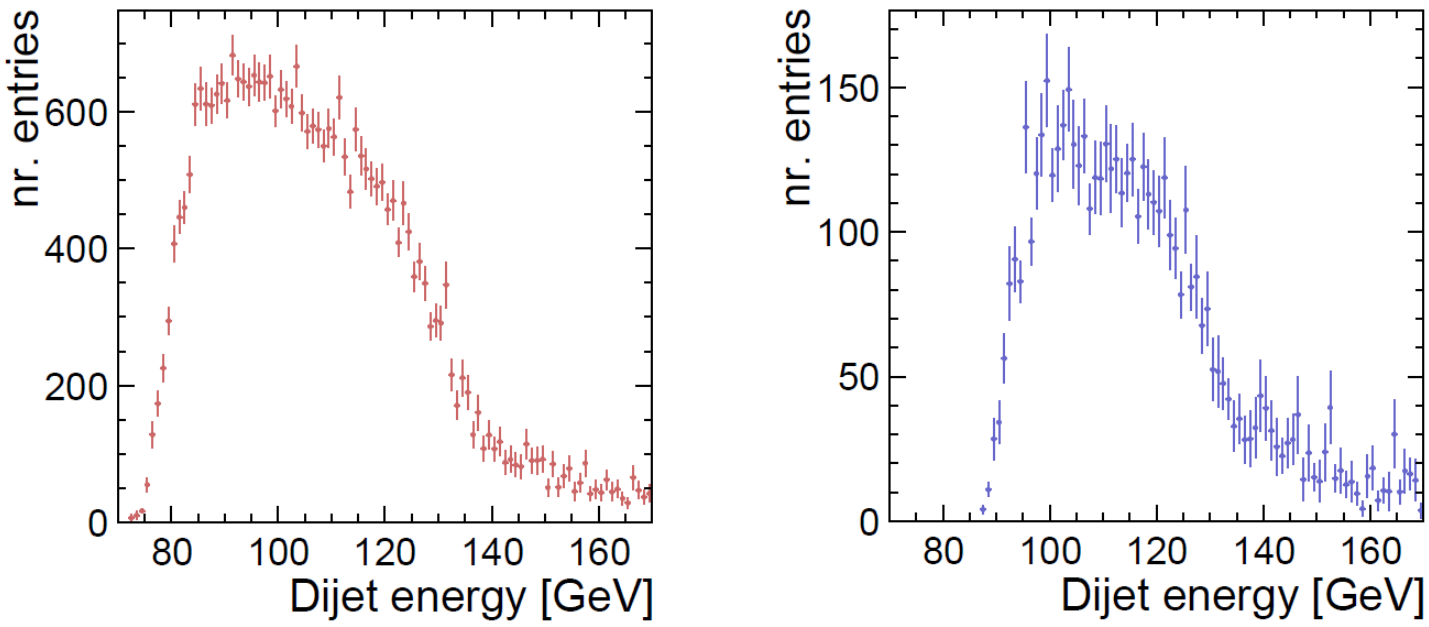

(a) $\tilde{\chi}_1^{\pm}$ candidates

(b) $\tilde{\chi}_2^0$ candidates

Figure 9: The di-jet energy spectra from the chargino (left) and neutralino (right) candidate events used in the kinematic edge extraction.

Section 5: Status

Edge Measurements with FIR Filters in the Point 5 Study Case

- Text is ready for review
- All figures produced with ILD – DBD full simulation Monte Carlo data (final)

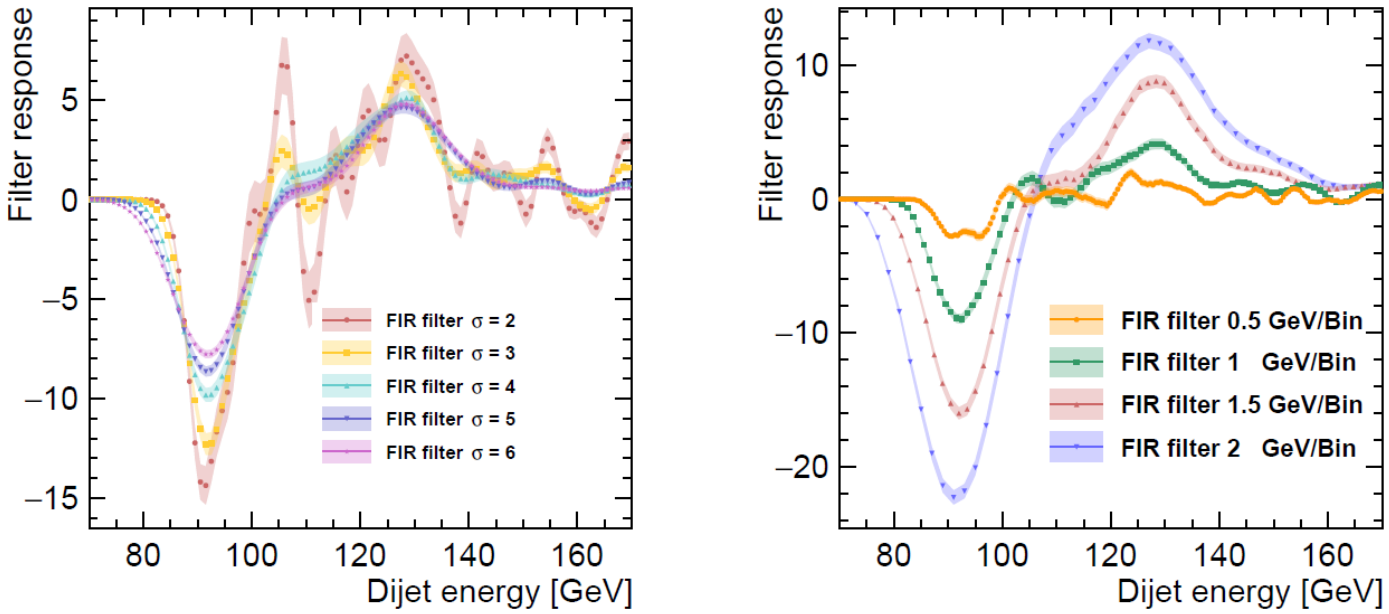

Figure 10: Filter responses obtained when varying the Gaussian σ parameter (left) and the input data binning (right) in the context of the optimisation procedure. The shown distributions were attained using the simulated $\tilde{\chi}_2^0$ candidate events. A very similar behaviour was observed in the case of the $\tilde{\chi}_1^{\pm}$ candidates.

Section 5: Status

Edge Measurements with FIR Filters in the Point 5 Study Case

- Text is ready for review
- All figures produced with ILD – DBD full simulation Monte Carlo data (final)

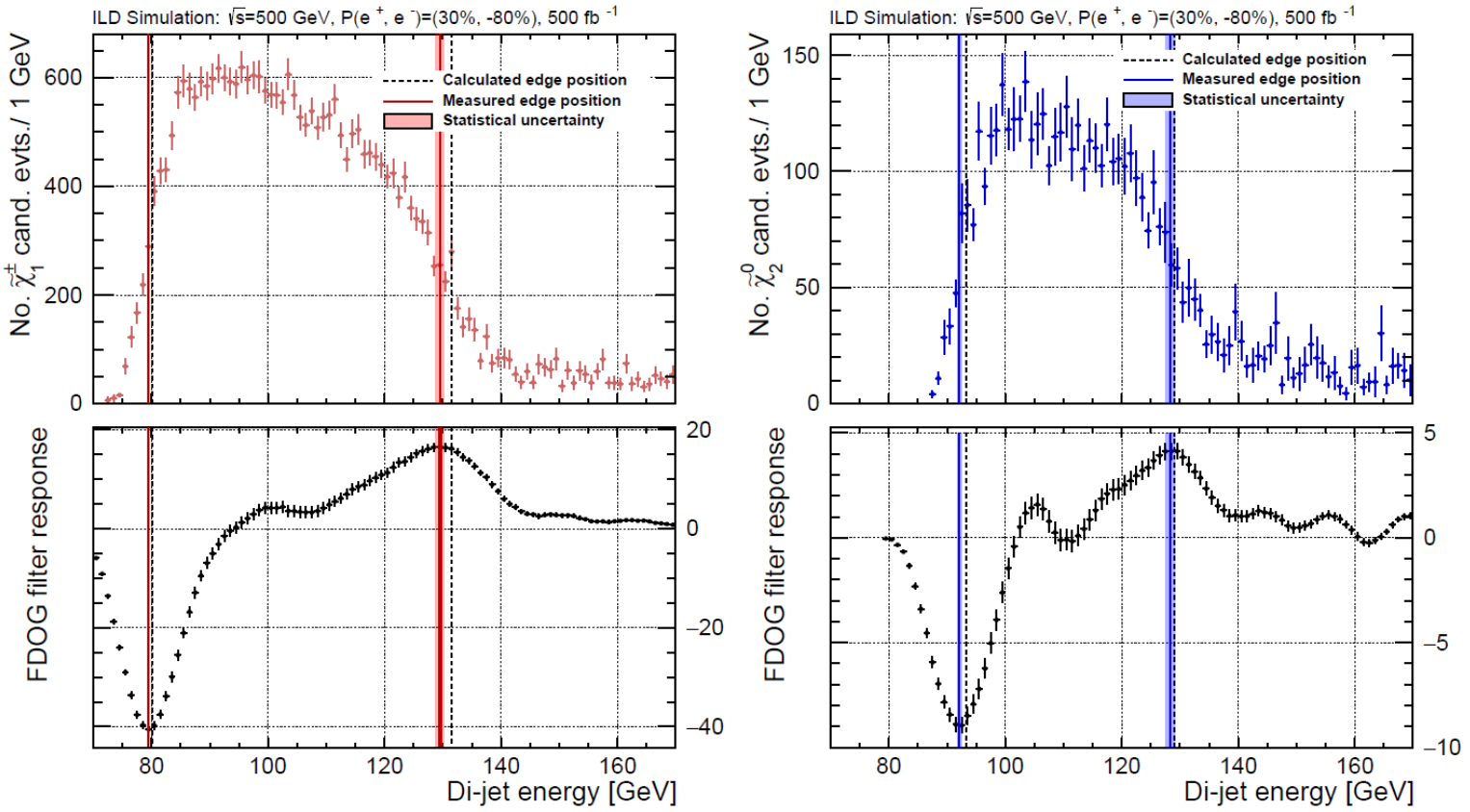

Section 5: Status

Edge Measurements with FIR Filters in the Point 5 Study Case

- Text is ready for review
- All figures produced with ILD – DBD full simulation Monte Carlo data (final)

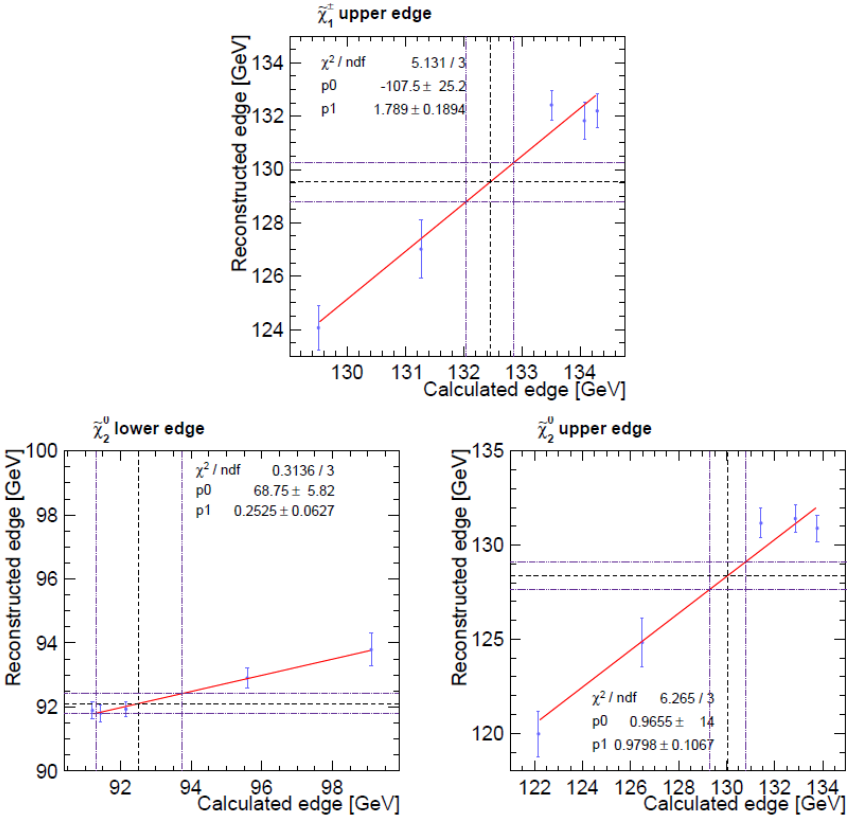

Figure 12: The edge position on reconstruction level versus the values calculated with formulae

Section 5: Final Results

Edge Measurements with FIR Filters in the Point 5 Study Case

- Measured edges:

	$\tilde{\chi}_1^{\pm}$ low [GeV]	$\tilde{\chi}_1^{\pm}$ high [GeV]	$\tilde{\chi}_2^{0}$ low [GeV]	$\tilde{\chi}_2^{0}$ high [GeV]
Calculated	80.17	131.53	93.24	129.06
FIR filter	79.5±0.2	129.5±0.7	92.1±0.3	128.4±0.8

- Perform edge calibration:

	$\tilde{\chi}_1^{\pm}$ high [GeV]	$\tilde{\chi}_2^{0}$ low [GeV]	$\tilde{\chi}_2^{0}$ high [GeV]
Calibrated	132.46 ± 0.44	92.52 ± 1.23	130.04 ± 0.77

- Final calculated masses:

	Mass $\tilde{\chi}_1^{\pm}$ [GeV]	Mass $\tilde{\chi}_2^{0}$ [GeV]	Mass $\tilde{\chi}_1^{0}$ [GeV]
Model	**216.5**	**216.7**	**115.7**
Mass w. calibration	214.1±4.8	216.9±3.4	115.5±1.8
Mass no calibration	216.7±3.1	220.4±1.3	118.1±0.9

Thank you

3. Study Cases

Overview

In particle physics: particle masses determined from kinematic edge location

- Considering direct searches for SUSY particles in R-parity conserving scenarios
  - **two body decay**: $\tilde{X} \rightarrow \tilde{Y}U$, where $\tilde{Y}$ is the stable LSP and U is a SM particle
  - momentum and energy conservation in rest frame of U:

$$p_U^2 = \frac{1}{4M_{\tilde{X}}^2}\left(\left(M_{\tilde{X}}^2 - M_{\tilde{Y}}^2 + M_U^2\right)^2 - 4M_{\tilde{X}}^2 M_U^2\right)$$

$$E_U = \frac{M_{\tilde{X}}^2 - M_{\tilde{Y}}^2 + M_U^2}{2M_{\tilde{X}}}$$

  - boost to lab frame:

$$E_U^{lab} = \gamma E_U + \beta\gamma \vec{p}_{U,\parallel}$$

$$= \gamma E_U + \beta\gamma |\vec{p}_U| \cos\theta'$$

$$\theta' = 0 \rightarrow E_U^{lab} = \gamma E_V + \beta\gamma\sqrt{E_V^2 - M_V^2}$$

$$\theta' = \pi \rightarrow E_U^{lab} = \gamma E_V - \beta\gamma\sqrt{E_V^2 - M_V^2}$$

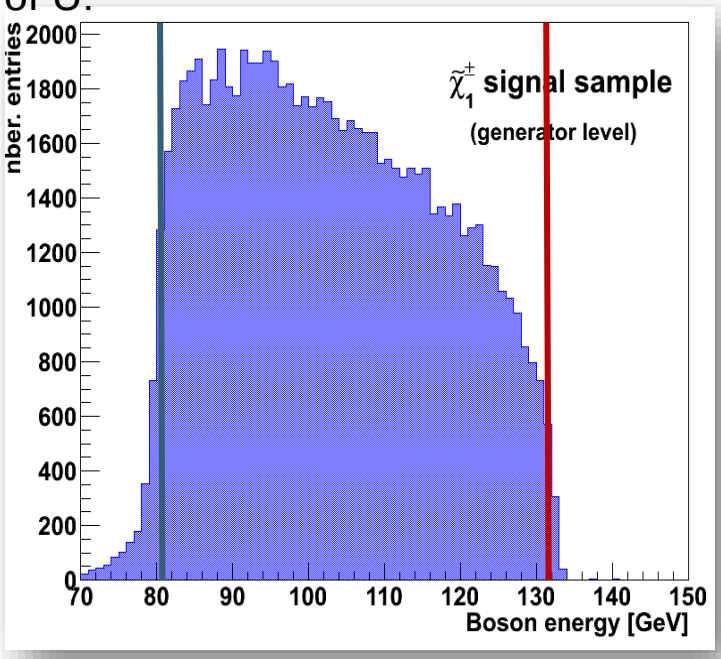

  - spin of involved particles determines shape of box top

2. A Computational Approach to Edge Detection

Overview

Define FIR filters & present their key elements for discrete input data:

- For continuous input data: $g(x)$; filter out noise before differentiation $f(x)$

$$\underbrace{R(x)} = \frac{d}{dx}(f(x) * g(x)) = \underbrace{\frac{df(x)}{dx}} * g(x) = h(x) * g(x)$$

Impulse response Matched filter = $h(x)$

- For discrete input data, e.g., histograms: $g_d(i)$; filter is also discrete $h_d(k)$

$$R_d(i) = \sum_{k=-N}^{N} h_d(k) \cdot g_d(i-k)$$; N = nr. coefficients after which resp. amplitude → 0

- Key "ingredients":
  - Mathematical expression of $h_d(k)$ = filter kernel
  - The filter size = N
  - Binning of the input histogram

2. A Computational Approach to Edge Detection

2.1. Optimisation Criteria for a Discrete Function Edge Finder

For continuous distributions: optimal filter ≈ first derivative of Gaussian (J.F. Canny, DOI:10.1109/TPAMI.1986.4767851) - True for discrete case as well?

- Reformulated Canny´s optimisation criteria:
  - efficiency
  - localisation error

  } discussed in detail in 3rd of July 2018 talk

- Considered 4 different potential functions:
  - Difference of boxes: $h_d(k) = \begin{cases} 1 \text{ for } -N \le k < 0 \\ 0 \text{ for } k = 0 \\ -1 \text{ for } 0 < k \le N \end{cases}$
  - First derivative of a Gaussian: $h_d(k) = -k\, e^{\frac{k^2}{2\sigma^2}}$
  - Deriche: $h_d(k) = -k\, e^{-\alpha|k|}$
  - Shen: $h_d(k) = \begin{cases} e^{\alpha k} & \text{for } -N \le k < 0 \\ 0 & \text{for } k = 0 \\ -e^{-\alpha k} & \text{for } 0 < k \le N \end{cases}$

FIR filter kernel for edge detection on binned distributions

- For continuous distributions: optimal filter ≈ **first derivative of Gaussian** (J.F. Canny, doi:10.1109/TPAMI.1986.4767851)
- Is this true for discrete distributions (i.e., histograms)? → S. Caiazza study

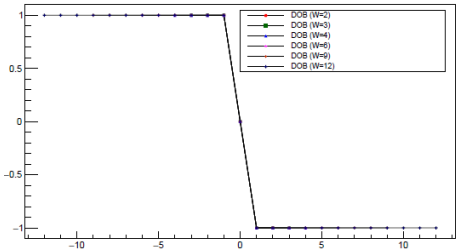

(a) DOB filter DIR

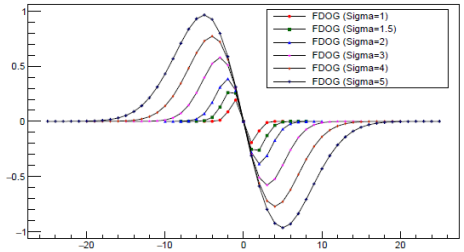

(b) FDOG Filter DIR

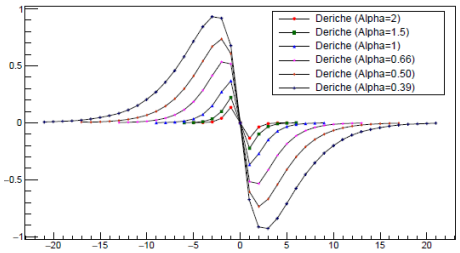

(c) Deriche Filter DIR

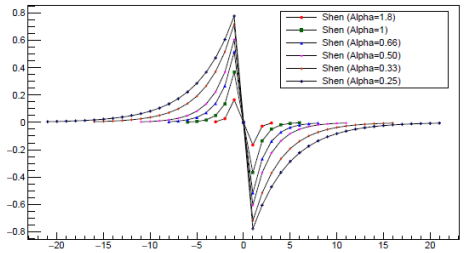

(d) Shen Filter DIR

Localisaion error and bias

- Evaluate performance of the 4 considered kernels in terms of:
  - Localisation error: σ_L

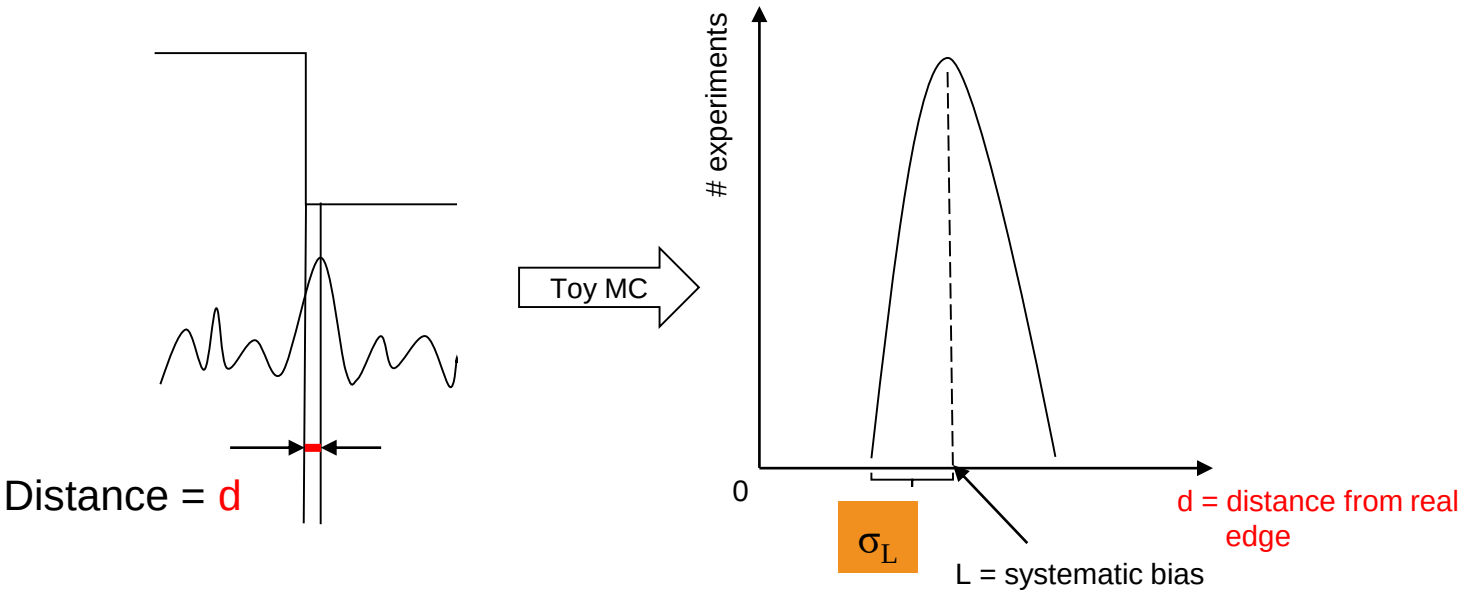

Two SUSY scenarios accessible at the ILC

- Illustrate the FIR filter method in the context of the ILC, using ILD simulated data:
  - Well known initial state → well defined kinematics
  - Handling of missing energy
  - High precision ↔ Particle Flow reconstruction

Investigating the FIR filter performance in two SUSY scenarios:

- selectron & gaugino pair production @ ILC: $\sqrt{s}$ = 500 GeV, $P(e^-)$ = -80%, $P(e^+)$ = +30%, 500 fb^{-1}
- Data sets
  - → **selectron analysis**: signal + SM & SUSY background simulated with SGV
  - → **gaugino analysis**: signal + SM & SUSY background simulated and reconstructed with DBD version of full simulation (ILD_o1_v5)

Edge Calibration

- Mass calculation formulae do not account for beam energy spectrum, gauge boson width, etc. effects on edge positions → **perform edge calibration**:
  - Vary input masses ↔ different edge positions
    → $\tilde{\chi}_1^{\pm}$ & $\tilde{\chi}_2^0$ varied simultaneously (210 GeV ↔ 225 GeV, 3 GeV step)
    → LSP mass fixed!
  - Measure edges for each new Monte Carlo sample
    → obtain **calibration curve**

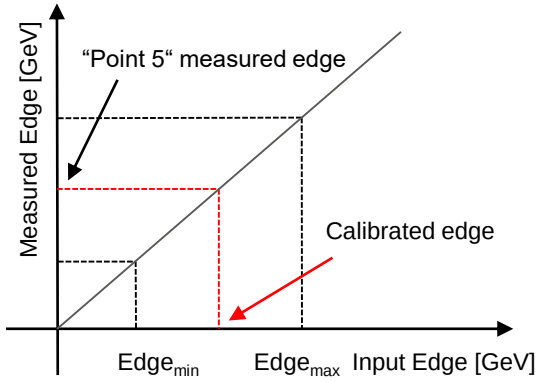

- Investigated 3 different aspects: calibrate edges measured on
  1. **generator level ↔ calculated edges:**
     effects of ISR emission, gauge boson width = 0.8% → 1.8%
  2. **reconstruction level ↔ generator level**
     simulation and reconstruction effects = **0.2% → 0.9%**
  3. **reconstruction level ↔ calculated edges**
     take all effects into account = 1.1% → 2%

	Mass $\tilde{\chi}_1^{\pm}$ [GeV]	Mass $\tilde{\chi}_2^0$ [GeV]	Mass $\tilde{\chi}_1^0$ [GeV]
Model	**216.5**	**216.7**	**115.7**
Mass w. calibration	214.1±4.8	216.9±3.4	115.5±1.8
Mass no calibration	216.7±3.1	220.4±1.3	118.1±0.9

Toy Monte Carlo Study – Fit Stability

Investigating the Stability of LOI Fit to Gauge Boson Energy Spectrum

- Randomly generated 10^4 $\tilde{\chi}_1^+$ and $\tilde{\chi}_2^0$ distributions + bgrd.
- Applied fit 10^4 times

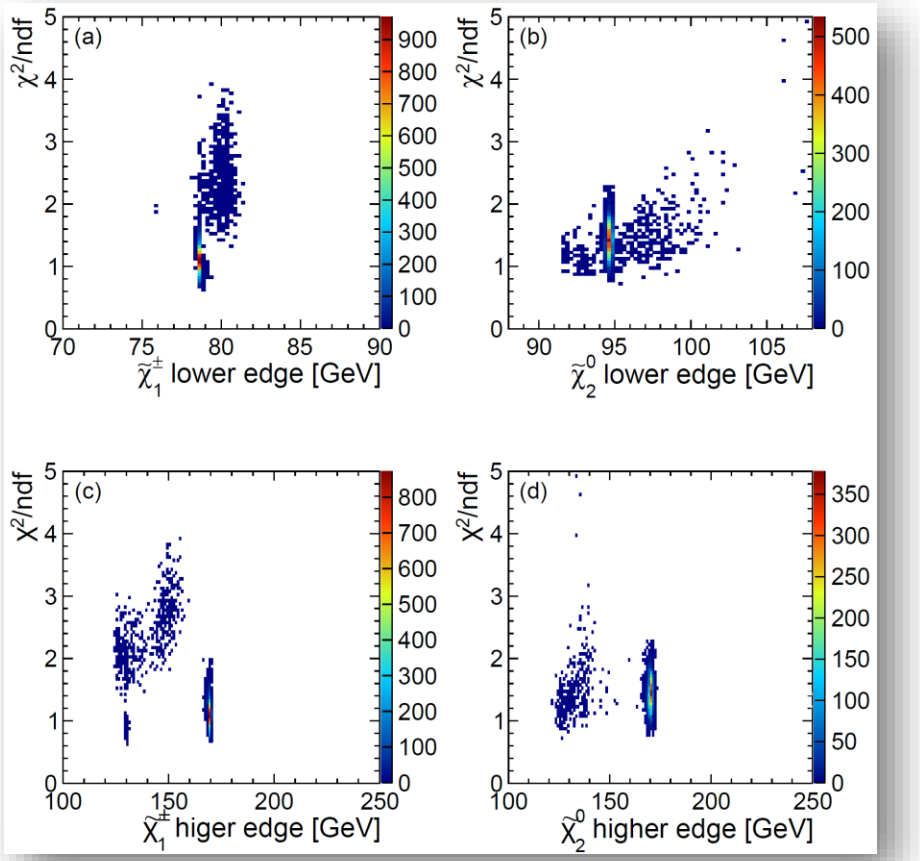

6. Conclusions

- Kinematic edge detection is crucial for determining particle masses in cases with large amounts of missing energy
- We propose a new method for kinematic edge detection: FIR filters
- The FDOG filter kernel was found to be optimal in the discrete case as well
- The FIR filter method was applied in the context of two different SUSY scenarios accessible at the ILC: STC4 and “Point 5”
- For each study case the kernel parameters were optimised
- Sparticles masses obtained from the FIR filter detected edges highly compatible with model masses & other methods
- FIR filter significantly more robust and stable